Peroxidation treatment of dye manufacturing wastewater in the presence of ultraviolet light and ferrous ions

Shyh-Fang Kang [a,*], Chih-Hsiang Liao [b], Hung-Pin Hung [a]

[a] *Department of Water Resources and Environmental Engineering, Tamkang University, Taipei, Taiwan*
[b] *Department of Environmental Engineering and Health, Chia-Nan College of Pharmacy and Science, Tainan, Taiwan*

Abstract

This study was performed to investigate the removal of COD and color from a dye manufacturing plant wastewater using the $H_2O_2/UV/Fe^{2+}$ process. Comparison of removal efficiencies were made among the H_2O_2/UV, the H_2O_2/Fe^{2+} and the $H_2O_2/UV/Fe^{2+}$ processes. Removal of COD and color of approximately 80 and 90% can be achieved by $H_2O_2/UV/Fe^{2+}$ processes, respectively. The H_2O_2/Fe^{2+} reaction is responsible for approximately 80% removal of both COD and color, the H_2O_2/UV reaction for 10%, and UV/Fe^{3+} for the remaining 10%. The removal kinetics of COD and color were consistent with those of H_2O_2 and Fe^{2+}, respectively. Ferrous ions addition at higher dosage results in the rate of COD removal per unit dosage higher than that of color, whereas the UV irradiation favors color removal more than the COD removal, in terms of rate or rate per unit power. It appears that there is some benefit gained by multi-step addition of Fe^{2+}, but not H_2O_2. © 1999 Elsevier Science B.V. All rights reserved.

Keywords: AOP; Dyestuffs; Photo-Fenton; Hydrogen peroxide

1. Introduction

Dye manufacturing wastewater normally has a high chemical oxygen demand (COD) as well as high color content, due to dye intermediates and auxiliary chemicals from the

---

* Corresponding author. E-mail: kangsf@ew001.ew.tku.edu.tw

process. Wastewater of this kind, if not appropriately treated, might pose a severe threat to receiving waters because of these chemicals, which are toxic to aquatic life [1] and may interfere with the light penetration as well. Given this concern, dye manufacturing industries are required to reduce both COD and color from their discharges. Combinations of conventional treatment processes, including coagulation, activated sludge oxidation, and chemical oxidation, have been commonly used by dye manufacturing industries in Taiwan. However, as the discharge regulations become more stringent, the treatment processes mentioned above appear to be inadequate to comply with the removal requirements of COD and color. Hence, advanced treatment facilities are urgently needed in this aspect.

This study attempts to utilize H_2O_2-based oxidation process with the addition of UV light and ferrous ions, which is known as an advanced oxidation process (AOP), for solving the problem noted above. H_2O_2 is a readily available chemical oxidant. H_2O_2 alone might not oxidize some refractory organics effectively. However, when H_2O_2 is catalyzed by UV light and ferrous ions, the reactions can lead to formation of an extremely reactive species in the solution, called the hydroxyl radical (HO ·), through the reaction pathways (See Fig. 1) such as Reaction Pathway (1): photolysis of hydrogen peroxide [2,3]; Reaction Pathway (2): Fenton's reaction [4]; Reaction Pathway (3): the photo-reduction of aquated ferric ions [5]; and Reaction Pathway (4): ferric ions-catalyzed decomposition of H_2O_2, which is then followed by heat- or UV-induced formation of ferrous ions and perhydroxyl radical [6,7]. The rates of Reaction Pathways (1) and (3) depend on the power of UV light. The rate constant of Reaction Pathway (2) was reported to be much larger than that of Reaction Pathway (4) by a factor of about 2650 [7]. The HO · radicals formed are capable of oxidizing target pollutants rapidly to achieve the treatment goal. Since the presence of UV light enhances the rate of HO · radicals formation through Reaction Pathways (1) and (3), the dosage of ferrous ions can be reduced, and thus the iron sludge problem can be mitigated.

As reported by many researchers, the advanced oxidation processes mentioned above were employed to remove or degrade successfully some refractory organics and color such as phenolic compounds [8–10], leachates [11], textile wastewaters [12–14], and dyestuff-contaminated wastewater [15]. The characteristics of both textile and dyestuff-contained wastewater is quite different from that of dye manufacturing wastewaters. So far, H_2O_2-based AOPs for treatment of dye manufacturing wastewater are rarely found in the literature [16].

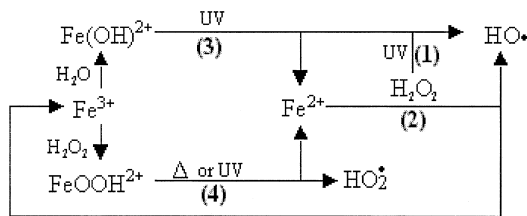The specific work in this study included first comparison of removal efficiencies of COD and color among the H_2O_2/UV, the H_2O_2/Fe^{2+} and the $H_2O_2/UV/Fe^{2+}$

Fig. 1. Schematic Reaction Pathways of HO · radical formation.

processes. Secondly, based on the use of $H_2O_2/UV/Fe^{2+}$ process, the effects of H_2O_2 and Fe^{2+} dosages, the UV power, and the multistep addition of H_2O_2 or Fe^{2+} on removal efficiencies were further investigated. As a result, this study provides dye manufacturing or related industries with valuable information regarding $H_2O_2/UV/Fe^{2+}$ as a promising process for wastewater treatment.

2. Experimental

2.1. Dye manufacturing wastewater characteristics

The wastewater samples used in this study were taken from the equalization tank of a dye manufacturing plant. The samples had a dark purple color and the light penetration depth was nearly zero. The main products manufactured in this plant belong to soluble reactive and acid dyes. Currently, the produced dye manufacturing wastewater is treated by chemical coagulation, activated sludge oxidation with powdered activated carbon, and chlorination. Due to new discharge standards in Taiwan, for example, COD < 100 mg/l, and American Dye Manufacturers Institute (ADMI) color value < 400, an advanced treatment unit is being considered in order to comply with the regulatory requirement. The original wastewater characteristics was as follows: ADMI color value = 29 200, COD = 6150 mg/l, chloride ion content (Cl^-) = 29 300 mg/l, suspended solids (SS) = 620 mg/l, and pH = 2.4. The samples to be treated by the experimental oxidation processes were obtained by diluting the above 18 times, resulting in: ADMI color value = 1100, COD = 350 mg/l, Cl^- = 1638 mg/l, SS = 35 mg/l, and pH = 3.5.

2.2. Process operation and water sampling

A batch photoreactor was utilized for this study, as shown in Fig. 2. An annular quartz reactor (9.5 cm i.d. and 35 cm height) with a liquid volume of approximately 2 l was placed in a photo-chamber, where a set of up to 16 low pressure mercury UV lamps (8 W each) were arranged in a circle surrounding the reactor. The UV light intensity had a wavelength of 254 nm primarily. After addition of predetermined amount of hydrogen peroxide and ferrous sulfate (both purchased from Merck) into the wastewater sample, the solution within the UV-irradiated reactor was stirred by a motor-driven mixer at a full speed to ensure homogeneous mixture. In addition, both sodium hydroxide and sulfuric acid were used to adjust pH at a constant value of 4.0 as desired in the experiment. As the reaction progressed, a sample volume of 50 ml was taken for the measurements of ADMI color value, COD, hydrogen peroxide, and ferrous ions at times of 0, 10, 30, 60, 90, and 120 min.

2.3. Chemical analysis

The detection of ADMI color value was based on ADMI Tristimulus Filter Method [17]. The light scan from 400 to 700 nm was performed using a spectrophotometer
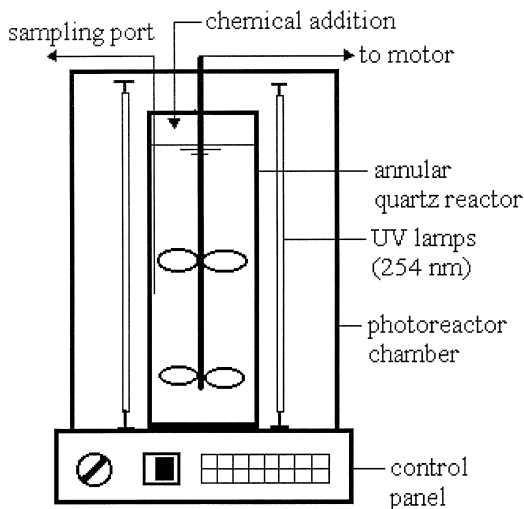
Fig. 2. Experimental set-up of photo-reactor.

(Hitachi U-2000). Thirty-one transmittance measurements for each treated solution were recorded at every 10 nm for further ADMI color value calculation using pre-installed computing software. The COD, which takes into account also the presence of H_2O_2 and/or Fe^{2+}, was measured using the procedure described in method 5220C in Standard Methods [17]. H_2O_2 was determined by potassium(IV) oxalate method [18] and the Fe^{2+} determined according to Standard Methods [17]. The experimental uncertainty was provided in the following. By diluting the original wastewater 20, 40, 80, and 160 times, respectively, the COD measurement was 6161 ± 103 (2%), and the color in ADMI unit was $33\,395 \pm 2578$ (8%). Two straight lines of standard calibration for residual H_2O_2 and Fe^{2+} measurement were obtained with the $R^2 = 0.9985$ and 0.9988, respectively.

3. Results and discussion

3.1. Process comparison on COD removal

It is known that HO · radical can be formed through different reaction pathways, as illustrated in Fig. 1. The relative contribution to HO · radical formation among reaction pathways is one of important issues to be examined in this study. Fig. 3 presents the comparisons of the COD removal by different processes, including H_2O_2/UV, H_2O_2/Fe^{2+}, and $H_2O_2/UV/Fe^{2+}$. This comparison can help one understand the enhancing effects of ferrous ions and UV light, respectively. In general, when the H_2O_2/UV process was employed, the addition of ferrous ions increased the COD removal by 36% at time of 10 min. In comparison, the UV-enhanced effect on the H_2O_2/Fe^{2+} process removal of COD showed an increase by 10% only at time of 10 min. In view of the initial removal rate of COD within the first 10 min, the rate ratio is
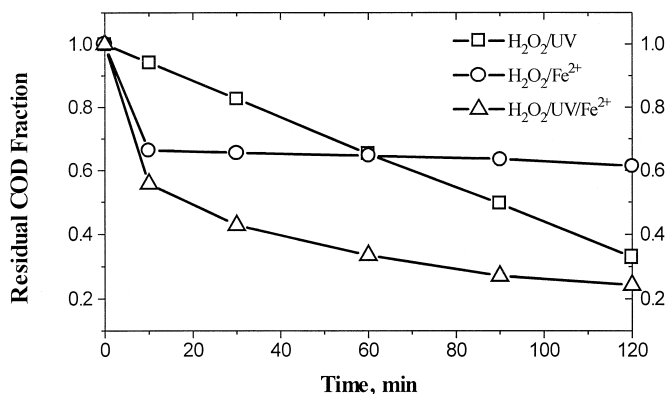
Fig. 3. Process performance comparison on the removal of COD: the initial $H_2O_2 = 680$ mg/l, the initial $Fe^{2+} = 105$ mg/l, the UV power = 128 W.

calculated as 0.13:0.76:1 in the sequence of H_2O_2/UV, H_2O_2/Fe^{2+}, and $H_2O_2/UV/Fe^{2+}$. The differences between the last value and the first two values describe the degree of enhancement in the presence of UV light and ferrous ions. According to the rate ratio, most HO$\cdot$ radical formation can be attributed to Reaction Pathway (2).

As the reaction continues from 10 to 120 min, further COD removal was observed to quite differ from one process to another. As shown in Fig. 3, the residual COD fractions for H_2O_2/UV, H_2O_2/Fe^{2+} and $H_2O_2/UV/Fe^{2+}$ processes were 94, 66, and 56% at 10 min, and they are 33, 61, and 24% at 120 min. For the H_2O_2/UV process, the COD removal at 10 min represents only 9% of the removal at 120 min, whereas they are 87% and 58% for H_2O_2/Fe^{2+} and $H_2O_2/UV/Fe^{2+}$ processes, respectively. These data indicate that the longer the reaction time, the more advantageous for COD removal in the H_2O_2/UV process, but not in the H_2O_2/Fe^{2+} process, which belongs to a relatively fast reaction. As for the $H_2O_2/UV/Fe^{2+}$ process, it tends to favor a longer reaction time under the condition of excessive H_2O_2. Similar results were also reported in the degradation of 2-nitrophenol by $H_2O_2/UV/Fe^{2+}$ process [9].

3.2. Process comparison on color removal

The profiles of residual color value fraction for the three processes were plotted in Fig. 4 under identical conditions as specified in Fig. 3. By contrast, the trends of color removal using H_2O_2/UV and H_2O_2/Fe^{2+} processes were found quite similar to those of COD removal, as shown in Fig. 4. But the color removal for $H_2O_2/UV/Fe^{2+}$ process appears to be significant only within the initial 10 min, and such a trend is quite different from that of COD removal, as indicated in Fig. 3, where a sharp decrease is observed. By calculating the initial rate of color removal within the initial 10 min, the ratio in the sequence of H_2O_2/UV, H_2O_2/Fe^{2+}, and $H_2O_2/UV/Fe^{2+}$ is as follows: 0.10:0.78:1, which is close to that of COD removal (0.13:0.76:1). By further calculating the relative color removal at the reaction times of 10 and 120 min for each process,
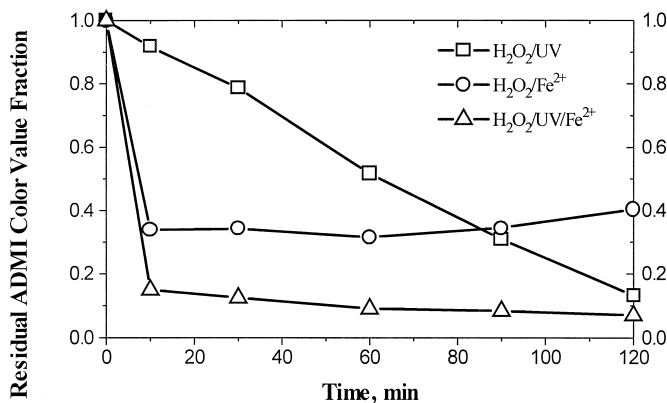
Fig. 4. Process performance comparison on the removal of ADMI color value: the initial $H_2O_2 = 680$ mg/l, the initial $Fe^{2+} = 105$ mg/l, the UV power = 128 W.

10%, 110%, and 92% in the sequence as mentioned before were obtained, respectively. Such a result indicates that a longer reaction time is not favorable to the color removal for both H_2O_2/Fe^{2+} and $H_2O_2/UV/Fe^{2+}$ processes, but favorable for H_2O_2/UV. It is noted here that the relative percentage of 110% (larger than 100%) is due to color increasing between 10 and 120 min.

According to the ratio data presented above, when the $H_2O_2/UV/Fe^{2+}$ process is used as a treatment technology for the studied wastewater, it might be inferred that Reaction Pathway (1) contributes 10% of the overall removal of both COD and color during the initial period, while Reaction Pathway (2) contributes 80%, and Reaction Pathways (3) and (4) together 10%. This result demonstrates that the presence of Fe^{2+} appears to be more beneficial than that of UV light, if iron sludge disposal problem is not taken into account.

3.3. Process comparison on H_2O_2 decomposition

Based on the same experimental conditions, as noted in Figs. 3–5 shows the behavior of H_2O_2 decomposition by different processes. The residual H_2O_2 fraction for H_2O_2/UV process was observed to decrease linearly with reaction time similar to the linear decreases of both residual COD and color fraction (see Figs. 3 and 4). As can be seen in Fig. 5, the consumption of H_2O_2 for H_2O_2/Fe^{2+} process represents about 30% of the initial amount within 10 min reaction, and only additional 10% consumption was obtained as the reaction proceeds until the time point of 120 min, where residual fraction of 60% was maintained. The remaining 40% was mainly due to the absence of ferrous ions after 10 min. The H_2O_2 decomposition in the H_2O_2/Fe^{2+} process can explain the reason why the COD and color removals occur mainly within the first 10 min, and then the removal becomes very limited after 10 min. In view of the above, evidence was also given that the studied dye manufacturing wastewater is resistant to H_2O_2 oxidation. Furthermore, since H_2O_2 reacts with Fe^{2+} very fast to form Fe^{3+} [19], and H_2O_2 is in
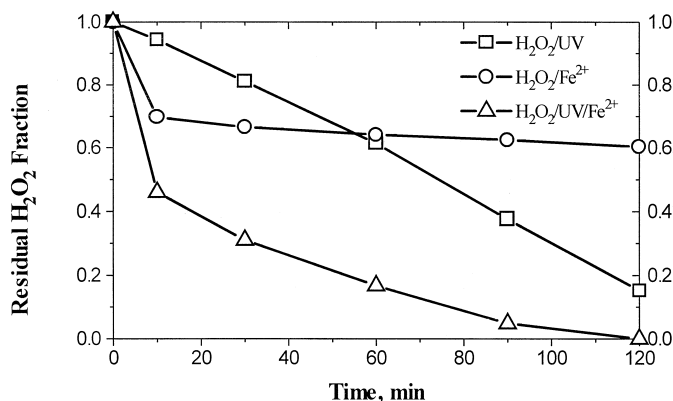
Fig. 5. Comparison of H_2O_2 decomposition by different processes: the initial $H_2O_2 = 680$ mg/l, the initial $Fe^{2+} = 105$ mg/l, the UV power = 128 W.

excess of Fe^{2+} in this case, it implies that ferric ions-catalyzed decomposition of H_2O_2, i.e. Reaction Pathway (4), can be neglected at the studied pH of 4.0.

Concerning the H_2O_2 decomposition for $H_2O_2/UV/Fe^{2+}$ process, Fig. 5 shows a dramatic residual change of approximately 50% within the first 10 min, and then gradually decreases down to a zero residue as the reaction progresses until the end. The latter reaction period of 110 min accounts for 50% decomposition of H_2O_2 mainly through UV photolysis, since that the ferrous ions have been fully consumed in the earlier reaction period of 10 min, and the ferric ions catalysis of H_2O_2 is not important. In spite of significant decomposition of H_2O_2 in the latter period, the amounts of the COD and color being removed appear to be quite different from each other. For example, it is shown that H_2O_2 decomposition in the latter period results in the increase of COD removal by 32% (see Fig. 3), whereas the increase of color removal was only by 8% (see Fig. 4). The reason is possibly due to the counteracting effect by the formation of reaction intermediates during the latter reaction period with color that are stronger than parent compound. For example, phenolic intermediates formed in the ferrioxalate-mediated photodegradation process were reported to absorb light in the region of 200–300 nm more strongly than their parent compounds of benzene, toluene, and xylenes [20]. Cyclohexanone shows no absorbance in the UV-range greater than 200 nm, but a small increasing absorbance maximum at 254 nm could be detected, when degraded in the Photo-Fenton process [21]. By comparison, the phenomenon of a slight color increase at the end of reaction was also observed in the H_2O_2/Fe^{2+} process (see Fig. 4).

As described above, $H_2O_2/UV/Fe^{2+}$ process has been shown to be more important than the other two processes in removing COD and color. The success of this process is primarily due to different sources of HO · radicals formation, as illustrated in Fig. 1. As can be understood, the amount of H_2O_2 dosage will control the process performance since the reaction pathway will be dominated by UV/Fe^{3+}, which is not an efficient source of HO · radicals, if the H_2O_2 is used up. The decision to utilize as much H_2O_2 as possible appears to be reasonable. However, as was in the case of H_2O_2/UV process

for removal of *n*-chlorobutane [22], increasing H_2O_2 dosage up to a certain point, the removal profile became stabilized for H_2O_2 dosage greater than that particular point. This result is believed to occur due to H_2O_2 itself being an effective HO · radical scavenger as well, the reaction rate constant of which was reported to be 2.7×10^7 M^{-1} s^{-1} [23]. Hence a proper dosage of H_2O_2 is critical in the $H_2O_2/UV/Fe^{2+}$ process, where the presence of Fe^{2+} further complicates the overall reactions. Two different H_2O_2 dosages were then applied so that they are equivalent to (Type I) and in excess of (Type II) Fe^{2+} dosage, respectively. The experimental results of their effect are described below.

3.4. Effect of low dosage ratio of H_2O_2 to Fe^{2+}

As shown in Fig. 6, when 340 mg/l of H_2O_2 and 110 mg/l of Fe^{2+} were utilized in the process, the residues of both were found near zero at 10 min. This implies that a molar ratio of H_2O_2 to Fe^{2+} at approximately 5 under the specified UV power is required to achieve a full consumption of both. In addition, from 10 min on, Fe^{2+} was regenerated gradually with time, due to the photoreduction of ferric ions and the absence of H_2O_2. As shown in Fig. 6, as high as 40 mg/l of Fe^{2+} or 36% of the initial amount was regenerated at 120 min. Note that if sufficient irradiation time is used, Fe^{2+} should reach its initial concentration via regeneration. Ruppert et al. (1993) reported a value of 90% recovery of Fe^{2+} over an irradiation period of approximately 7 h [24].

Concerning the residues of COD and color based on equivalent concentration ratio of Type I, Fig. 7 shows two profiles in 'L' shape with the minimum values of 40% and 15% at 10 min, respectively. When the reaction time was extended, the COD residue remained rather unchanged for the rest of reaction time, since HO · radical precursor H_2O_2 is already absent in the solution, and unfortunately the HO · radical formation through photoreduction of ferric ions is minor. On the other hand, the color residue was observed to have a slight increase between times of 10 and 120 min, which might be due
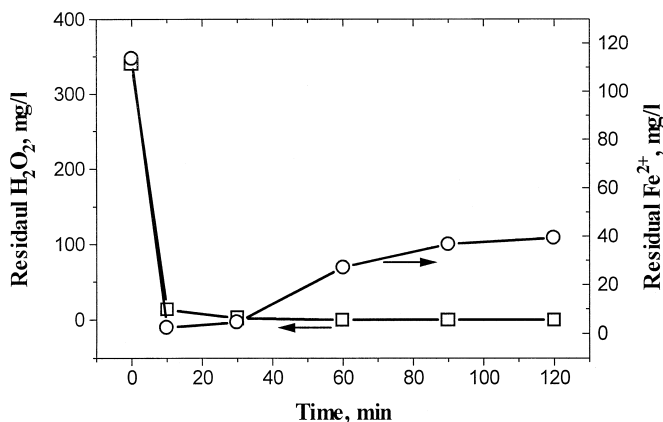

Fig. 6. Residual relationship between H_2O_2 and Fe^{2+} (Type I): the initial $H_2O_2 = 340$ mg/l, the initial $Fe^{2+} = 110$ mg/l, the UV power $= 128$ W.
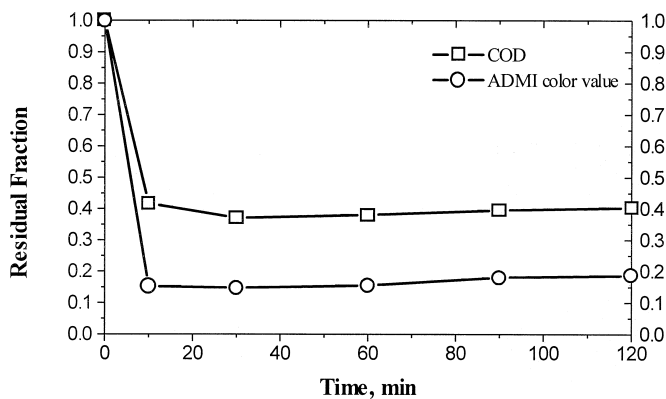
Fig. 7. Effect of the relative conc. ratio of H_2O_2 versus Fe^{2+} on the removal of COD and color (Type I): the initial $H_2O_2 = 340$ mg/l, the initial $Fe^{2+} = 110$ mg/l, the UV power $= 128$ W.

to the regeneration of color-contributing species such as ferrous ions, as can be seen in Fig. 7. Kang and Chang reported that after H_2O_2/Fe^{2+} treatment of textile wastewater the color residue tends to increase with especially the higher dosage of ferrous ions at the end of reaction [14].

3.5. Effect of high dosage ratio of H_2O_2 to Fe^{2+}

By adding an excess of H_2O_2, Figs. 8 and 9 show the residual profiles totally different from those in Figs. 6 and 7. The gradually decreasing trends of H_2O_2 and COD residues in Figs. 8 and 9, respectively, are in sharp contrast to the L-shape lines of both residues in Figs. 6 and 7. On the other hand, as shown in Fig. 8, the initial Fe^{2+} of
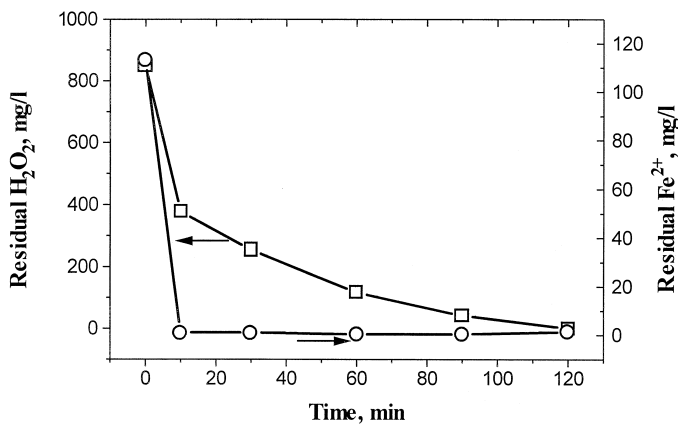

Fig. 8. Residual relationship between H_2O_2 and Fe^{2+} (Type II): the initial $H_2O_2 = 850$ mg/l, the initial $Fe^{2+} = 110$ mg/l, the UV power $= 128$ W.
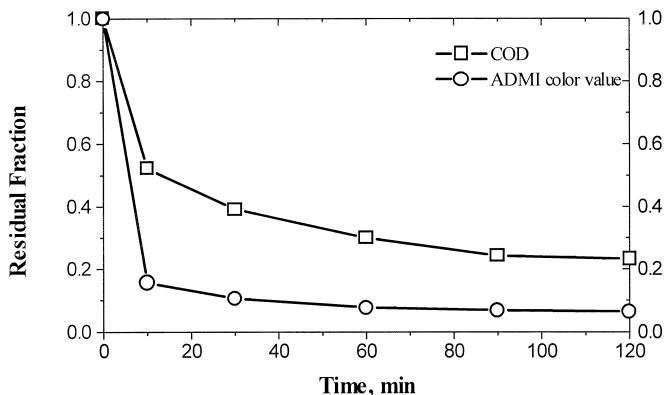
Fig. 9. Effect of the relative conc. ratio of H_2O_2 versus Fe^{2+} on the removal of COD and Color (Type II): the initial $H_2O_2 = 850$ mg/l, the initial $Fe^{2+} = 110$ mg/l, the UV power $= 128$ W.

110 mg/l was consumed completely after 10 min reaction, and its residue was zero value throughout the latter reaction period, since sufficient residue of H_2O_2 is still present in the solution and thus suppresses the regeneration of Fe^{2+}, given the initial H_2O_2 of 850 mg/l.

As for the color removal in the case of Type II (see Fig. 9), the first 10 min account for around 85% removal, and then show a slight removal of approximately 10% for the rest of reaction period, which contrasts a slight increase in color in the case of Type I (see Fig. 7).

To summarize the results from Figs. 6–9, the removal kinetics of COD and color in the $H_2O_2/UV/Fe^{2+}$ process were consistent with those of H_2O_2 and Fe^{2+} residues, respectively, regardless of different concentration ratios of H_2O_2 and Fe^{2+}. In addition, the process reactions for the case of Type I proceed first with fast Reaction Pathways (1) and (2) and then divert to a slow Reaction Pathway (3). For the case of Type II, the process reactions begin with Reaction Pathways (1) and (2), and afterwards Reaction Pathway (2) is suppressed due to the absence of ferrous ions, leaving Reaction Pathway (1) and (3) to carry on the reaction.

3.6. Effect of Fe^{2+} dosage

Since ferrous ions catalyze H_2O_2 to form HO · radical quite quickly, it seems also advantageous to utilize ferrous ions as much as possible. However, the HO · radical may be scavenged by ferrous ions with a rate constant of as high as 3.3×10^8 M^{-1} s^{-1} [23]. Hence, it is not necessarily true that ever-increasing ferrous ions dosage will result in proportional removal of COD and color from the wastewater. To justify this argument, the experiments were performed to examine the initial rates of COD and color removal at time of 10 min against Fe^{2+} concentration ranging from 0 to 220 mg/l.

As illustrated in Fig. 10, the initial color removal rate is seen to increase with the ferrous dosage remarkably in the lower end, beginning with the absence of ferrous ions. But it then tends to remain unchanged, and even a slight decrease is found in the higher
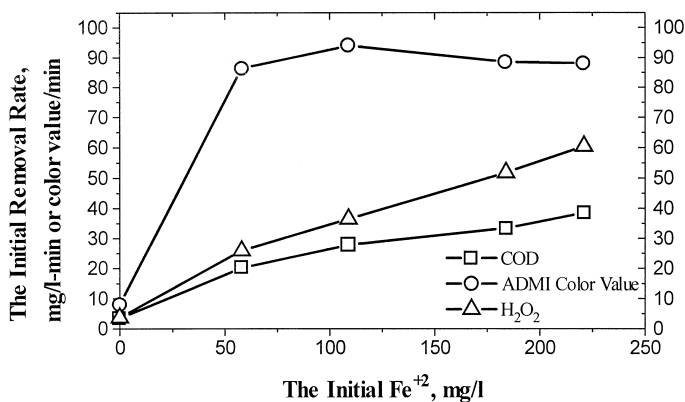
Fig. 10. Effect of ferrous ions on the $H_2O_2/UV/Fe^{2+}$ process: the initial $H_2O_2 = 666$ mg/l, the UV power = 128 W, the reaction time = 10 min.

end, due to formation of iron-contained color species, as has been discussed earlier. Zhu et al. reported that the initial reaction rate of H-acid organics in the H_2O_2/Fe^{2+} process decreases, when the ferrous dosage is more than a certain level [16]. On the other hand, both the initial rates of COD removal and H_2O_2 decomposition increased throughout the reaction period. In comparison, the rate of color removal was approximately 2 to 4 times of the COD removal under different Fe^{2+} dosages. However, in view of removal rate per unit Fe^{2+} dosage, the rate of COD removal appears to be more significant than the color removal, when the Fe^{2+} concentration is larger than 60 mg/l, as compared from the tangent slope.

3.7. Effect of UV power

According to Fig. 1, UV light in the $H_2O_2/UV/Fe^{2+}$ process plays the roles of photolysis of H_2O_2 and photoreduction of ferric ions, which lead to the formation of HO · radicals. The primary quantum yield of HO · radicals at 254 nm for the former was reported to be 1.0 [2,3], while the quantum yields at 313 and 360 nm for the latter were 0.14 and 0.017, respectively [5]. Since UV light at 254 nm was used in this study, the quantum yield for ferric photolysis was expected to be more than 0.14, knowing that its quantum yield increases with decreasing wavelength. At any rate, the aquated ferric ions still cannot compete with H_2O_2 for light photons in a significant way. However, when the H_2O_2 is fully consumed, the reaction of UV light-irradiated ferric ions becomes important. In consideration of these, it is always desirable to shed light on the UV effects on the removals of COD and color.

Fig. 11 shows the UV power affecting the initial removal rates of COD and color in a quite different way. The initial rate of color removal is observed to be much higher than that of COD under all different UV powers. In view of the rate removal per unit UV power, i.e. the tangent slope, the UV application seems to favor color removal more than COD as well. Furthermore, the increase of UV power by a factor of approximately 2.7 results in increases of initial removal rates of COD, color and H_2O_2 only by a factor of
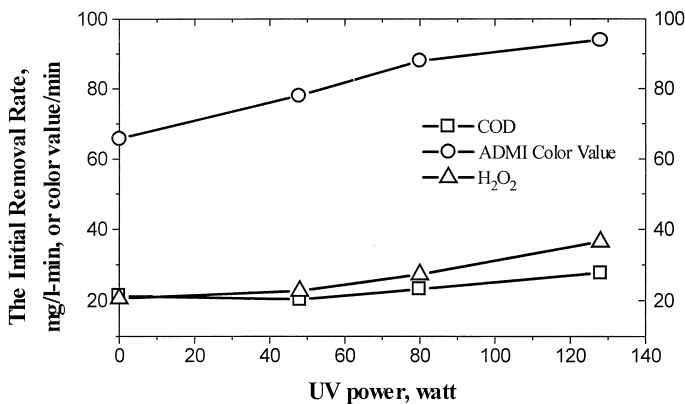
Fig. 11. Effect of UV power on the H_2O_2 /UV/Fe^{2+} process: the initial $H_2O_2 = 666$ mg/l, the initial $Fe^{2+} = 108$ mg/l, the reaction time $= 10$ min.

1.3, 1.4, and 1.6, respectively, according to the data presented in Fig. 11. These data also indicate that application of a very high level of UV power in the process of H_2O_2/UV/Fe^{2+} as a strategy to accelerate the initial removal rates of COD and color for the studied wastewater is not economically efficient, since light photons catalyze H_2O_2 to decompose only slowly. A similar result was also reported for the removal of *n*-chlorobutane from the humic substance-contained natural water using H_2O_2/UV process [25]. Hence, to gain benefit from increasing UV power in the process of H_2O_2/UV/Fe^{2+}, a considerable reaction time appears to be a prerequisite, allowing enough time for photoreduction of ferric ions to occur. For example, Ruppert at al. reported that Photo-Fenton degradation of TOC for two different UV powers showed no significance difference in the first hour, but the difference became greater for the latter reaction period of as long as 6 h [24].

3.8. Multi-step addition of H_2O_2

As shown in Figs. 6–9, the mechanism of COD and color removal in the H_2O_2/UV/Fe^{2+} process can be revealed by the residues of H_2O_2 and Fe^{2+}. These residues in turn depend on the method of chemical addition, for example, one-step or multi-step addition, thus affecting the process performance. Multi-step addition of chemical was considered due to that the initial application of one reactant might be in excess of the other. To avoid the excessive application or rather the waste of chemical, the step addition appears to be attractive. Bowers et al. [26] and Mohanty and Wei [27] used the H_2O_2/Fe^{2+} process for degradation of toxic organics and reported that multi-step addition of H_2O_2 shows a removal efficiency better than one-step addition, without further explanation of cause and effect. Hence, it is also desirable to know if the multi-step addition of H_2O_2 or Fe^{2+} will lead to any improvement on the performance of H_2O_2/UV/Fe^{2+} process.

Figs. 12–14 present the comparison of one-step and four-step additions of H_2O_2, in terms of residues of COD, color, H_2O_2 and Fe^{2+}. The amount of H_2O_2 applied was
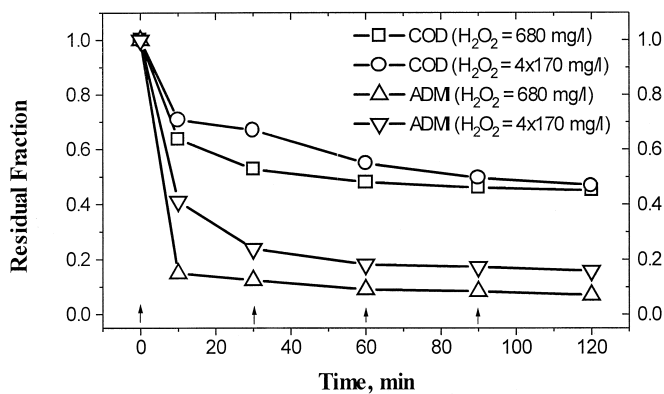
Fig. 12. Effect of step addition of H_2O_2 on the $H_2O_2/UV/Fe^{2+}$ process performance: the initial $Fe^{2+} = 140$ mg/l, the UV power = 128 W.

680 mg/l in one-step addition, and 170 mg/l in four-step addition at times of 0, 30, 60, and 90 min. As shown in Fig. 12, the residual fractions of COD and color at reaction time of 10 min in the case of one-step addition were approximately 65 and 15%, respectively, which were compared to 70 and 40% in the case of four-step addition. After a reaction time of 120 min, the residues for the case of one-step addition were lower than the case of four-step addition. In view of the plot of Fe^{2+} against time, Fig. 13 shows almost zero residues for both cases after 10 min. This indicates that both Reaction Pathway (1) and (2) (see Fig. 1) were important within the first 10 min, however, it was only Reaction Pathway (1) that was responsible for the removals of COD and color after 10 min. Such a phenomenon can be further demonstrated in Fig. 14, which shows the H_2O_2 residue against time in both cases. In the case of one-step addition, the H_2O_2 residue decreases from 680 to 315 mg/l rapidly within the first 10 min, and it then decreases gradually after 10 min, which was found similar to a linear trend of H_2O_2/UV process, as illustrated in Fig. 5.
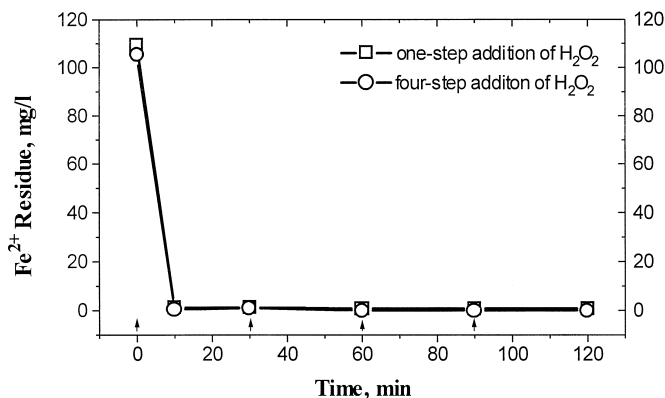

Fig. 13. Effect of step addition of H_2O_2 on the Fe^{2+} residue: the initial $Fe^{2+} = 140$ mg/l, the UV power = 128 W.
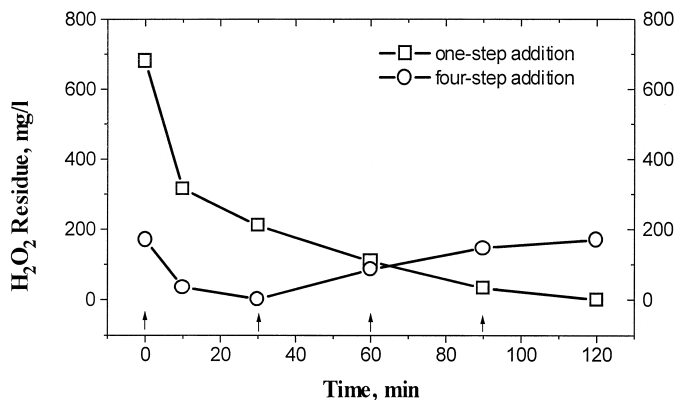
Fig. 14. Effect of step addition of H_2O_2 on the H_2O_2 residue: the initial $Fe^{2+} = 140$ mg/l, the UV power = 128 W.

In contrast, when the H_2O_2 was added at four different times, the H_2O_2 residue decreases from the initial of 170 to 36 mg/l and to almost zero mg/l at 10 and 30 min, respectively. In addition, within the time period between 10 and 30 min, COD and color were removed with low efficiency. This was because both H_2O_2 and Fe^{2+} concentrations have approached almost to zero within that period, and unfortunately the left Reaction Pathways (3) and (4) belong to slow reactions. Thus the timing of chemical addition needs to be carefully evaluated and continuous addition of chemical may be a better way to maximize the process performance. After the second, third, and fourth additions of H_2O_2, the residue was observed to accumulate with time, and the final residue was measured approximately 170 mg/l. One then concluded that the H_2O_2 consumed was 510 mg/l within the overall reaction time of 120 min, which was compared to the consumption of 680 mg/l in the case of one-step addition. The difference of H_2O_2 consumption between both cases of addition can be due to inefficient work during the period near the time point of the next addition, as just described above. To summarize, it was found that there seems no benefit to be gained by adding H_2O_2 in multi-step addition in the process of $H_2O_2/UV/Fe^{2+}$, which is contrary to the reported result in the H_2O_2/Fe^{2+} process [26,27].

3.9. Multi-step addition of Fe^{2+}

Concerning the step addition of Fe^{2+}, Figs. 15–17 present the residual profiles of COD, color, Fe^{2+}, and H_2O_2 under the conditions of one-step and four-step additions of Fe^{2+}. Similarly, the Fe^{2+} added was 140 mg/l in one-step addition and 35 mg/l in four-step addition at times of 0, 30, 60, 90 min. As shown in Fig. 15, the residual fractions of COD and color were approximately 62 and 15% at 10 min in the case of one-step addition of Fe^{2+}. These fractions were compared to 67 and 40% for COD and color residues, respectively in the case of four-step addition. On the other hand, the residual H_2O_2 fractions was found to be 31% in the former case and 50% in the latter case, as show in Fig. 17. The higher removal of both COD and color in one-step
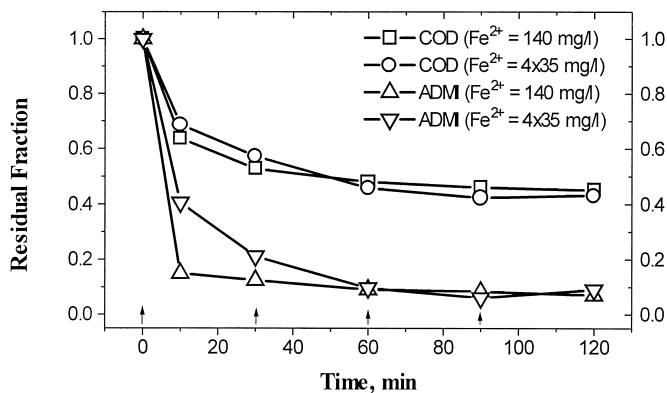
Fig. 15. Effect of step addition of ferrous ions on the $H_2O_2/UV/Fe^{2+}$ process performance: the initial $H_2O_2 = 680$ mg/l, the UV power = 128 W.

addition can be depicted due to the larger amount of H_2O_2 consumption within the first 10-min period. In addition, Fig. 16 shows that the Fe^{2+} residues became almost zero after 10 min in one-step addition, indicating that Reaction Pathway (2) is no longer important and Reaction Pathway (1) is left to be responsible for any removal of COD or color beyond that point.

As illustrated in Fig. 15, the removal of COD and color in the time period of 60 to 90 min were slightly better in four-step addition than in one-step addition, as is reverse within the initial range of 30 min. When the reaction lasts from 90 until 120 min, the difference of removal appears to be becoming insignificant. The reason is due to that the residual H_2O_2 has been almost consumed completely at 90 min in the case of four-step addition (see Fig. 17), and thus leaving the fourth addition of 35 mg/l of Fe^{2+} of no avail. This conclusion is also evidenced by the accumulation of Fe^{2+} residue in the time
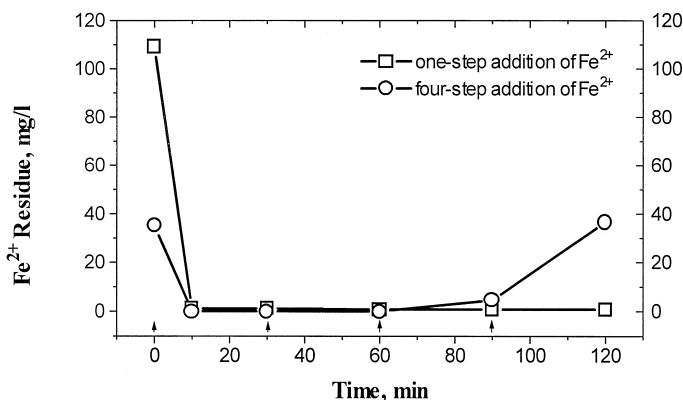

Fig. 16. Effect of step addition of ferrous ions on the Fe^{2+} residue: the initial $H_2O_2 = 680$ mg/l, the UV power = 128 W.

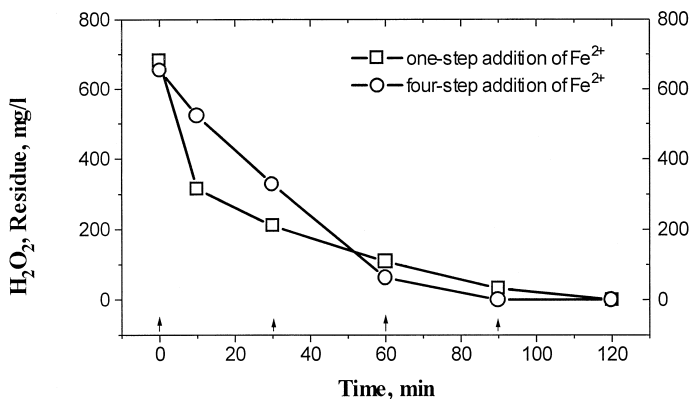Fig. 17. Effect of step addition of ferrous ions on the H_2O_2 residue: the initial $H_2O_2 = 680$ mg/l, the UV power $= 128$ W.

period of 90 to 120 min (see Fig. 16). Hence this result implies that only three additions of Fe^{2+} are sufficient to achieve identical efficiency and thus the fourth addition can be avoided. In summary, the multi-step addition of Fe^{2+} tends to perform better in the stage of latter reaction period, and may save some of Fe^{2+} compared to one-step addition. This finding was somehow different from the step addition of Fe^{2+} in the process of H_2O_2/Fe^{2+} for the treatment of 2,4-dinitrotoluene, which reported the opposite result [27].

4. Conclusion

In conclusion, this study provides a comparison on the removal of COD and color from a dye manufacturing plant wastewater among H_2O_2/UV, H_2O_2/Fe^{2+} and $H_2O_2/UV/Fe^{2+}$ processes. For the removal of COD and color in the $H_2O_2/UV/Fe^{2+}$ process, approximately, H_2O_2/Fe^{2+} reaction accounts for 80%, H_2O_2/UV 10%, and the photoreduction of ferric ions the remaining 10%. In particular, the $H_2O_2/UV/Fe^{2+}$ process was chosen for further study on the effects of process parameters such as hydrogen peroxide and ferrous dosages, and UV power on the process performance. In general, the efficiency of 80% can be achieved for COD removal within 2 h reaction time, and 90% for color removal. The $H_2O_2/UV/Fe^{2+}$ process favors a longer reaction time in COD removal but not in color removal, when the H_2O_2 is present in excess of Fe^{2+}. The residual profile of COD was found similar to that of H_2O_2 decomposition, and the residual color profile similar to that of Fe^{2+} residue. The effect of Fe^{2+} at higher dosage was found to be significant on the initial removal rate of COD per unit dosage, but not on color removal, possibly due to formation of iron-contained color species. Increasing UV power appears to be favorable in color removal more than in COD removal, however, application of a higher UV power is not a justifiable practice, unless process reaction lasts long enough. In consideration of multi-step addition of either H_2O_2 or Fe^{2+}, there was some benefit gained in the case of four-step addition of Fe^{2+} but not in the case of H_2O_2.

Acknowledgements

References

[1] J. Cooper, J. Soc. Dyers Color 18 (4) (1992) 176.
[2] J.H. Baxendale, J.A. Wilson, Trans. Faraday Soc. 53 (1956) 344.
[3] D.H. Volman, J.C. Chen, J. Am. Chem. Soc. 81 (1959) 4141.
[4] H.J.H. Fenton, Chem. Soc. J. (London) 65 (1894) 899.
[5] B.C. Faust, J. Hogine, Atmospheric Environ. A 24 (1) (1990) 79.
[6] J.J. Pignatello, Environ. Sci. Technol. 26 (1992) 944.
[7] Y. Sun, J.J. Pignatello, Envrion. Sci. Technol. 27 (1993) 304.
[8] C.P. Huang, C.D. Dong, Z.H. Tang, Waste and Management 13 (5/7) (1993) 361.
[9] J. Kiwi, C. Pulgarin, P. Peringer, Appl. Catal. B: Environ. 3 (1994) 335.
[10] J. Chen, W.H. Rulkens, H. Bruning, Wat. Sci. Technol. 35 (4) (1997) 231.
[11] S.M. Kim, S.U. Geissen, A. Vogelpohl, Wat. Sci. Technol. 35 (4) (1997) 239.
[12] S.H. Lin, C.F. Peng, Environ. Technol. 16 (1995) 693.
[13] N. Deng, F. Wu, F. Luo, Z. Liu, Chemosphere 35 (11) (1997) 2697.
[14] S.F. Kang, H.M. Chang, Wat. Sci. Technol. 36 (12) (1997) 215.
[15] E.G. Solozhenko, N.M. Soboleva, V.V. Goncharuk, Wat. Res. 29 (9) (1995) 2206.
[16] W.P. Zhu, Z.H. Yang, L. Wang, Wat. Res. 30 (12) (1996) 2949.
[17] American Public Health Association, American Water Works Association, Water Environment Federation, Standard Methods for the Examination of Water and Wastewater, 19th edn., Washington, DC, USA, 1995.
[18] R.M. Sellers, Analyst 105 (10) (1980) 950.
[19] Y. Zuo, J. Hoigne, Environ. Sci. Technol. 26 (5) (1992) 1014.
[20] A. Safarzadeh-Amiri, J.R. Bolton, S.R. Cater, Wat. Res. 31 (4) (1997) 787.
[21] G. Ruppert, R. Bauer, G. Heisler, S. Novalic, Chemosphere 27 (8) (1993) 1339.
[22] C.H. Liao, M.D. Gurol, Enviro. Sci. Technol. 29 (12) (1995) 3007.
[23] G.V. Buxton, C.L. Greenstock, W.P. Helman, A.B. Ross, J. Phys. Chem. Ref. Data 17 (1988) 513.
[24] G. Rupert, R. Bauer, G. Heisler, J. Photochem. Photobiol. A: Chem. 73 (1) (1993) 75.
[25] C.H. Liao, The Investigation of Hydrogen Peroxide Photolysis As A Water Treatment Process, PhD dissertation, Drexel University, Philadelphia, PA, 1993.
[26] A.R. Bowers, P. Gaddipati, W.W. Eckenfelder Jr., R.M. Monsen, Wat. Sci. Technol. 21 (6) (1989) 477.
[27] N.R. Mohanty, I.W. Wei, Hazardous Waste and Hazardous Mater. 10 (2) (1993) 171.